CrystEngComm

ROYAL SOCIETY OF CHEMISTRY

COMMUNICATION

View Article Online
View Journal

Cite this: DOI: 10.1039/d6ce00126b

Received 9th February 2026,
Accepted 20th April 2026

DOI: 10.1039/d6ce00126b

rsc.li/crystengcomm

Stepwise introduction of dipole blades into triptycenes: opening the variety of crystalline molecular packing modes

Hikaru Yamamoto,[a] Yoshichika Tsubakihara,[b] Ayana Sato-Tomita[c] and Mingoo Jin *[d]

We report that the stepwise introduction of difluorophenylene as dipolar blades into triptycenes diversifies the intermolecular packing modes in crystals. Single crystal XRD studies revealed that changing the number of dipoles in triptycene tunes the intermolecular packing from two dimensional intermeshed structures to helical structures, offering a novel insight for engineering triptycene-based supramolecular materials.

Triptycene is a rigid, tripodal molecule composed of three phenylene blades, which gives it a unique three-dimensional topology.[1] Owing to its structural rigidity and high symmetry, triptycene readily forms highly ordered supramolecular architectures in the solid state, such as intermeshed frameworks and channel-like porous networks.[2,3] These characteristic packing motifs have enabled the development of various functional materials, ranging from porous solids to organic thin-film devices.[3,4]

The packing behavior of triptycene can be tuned by introducing substituents that modify its steric environment and electronic characteristics, thereby influencing intermolecular interactions such as hydrogen bonding,[5–23] π–π stacking,[5,7,24–29] CH–π interactions,[8,21] and σ-hole interactions.[30,31] Although such modifications often lead to diverse crystal packing modes, it remains challenging to rationally control the resulting intermolecular arrangements because the prediction of packing structures from molecular information is inherently difficult. In addition to steric effects at the molecular level, electronic factors—such as molecular dipoles—can also serve as parameters to modulate intermolecular packing. In particular, fluorine substitution can tune electronic properties and enhance dipole moments while leaving the molecular framework largely unchanged.[32] Despite this potential, the influence of fluorine substitution on the packing and assembly of triptycene-based systems remains unexplored.

In this study, we investigated how the stepwise introduction of a 2,3 difluorophenylene moiety as a dipolar blade, which reduces the dramatic change of steric bulkiness, affects the intermolecular packing of triptycene derivatives in crystals. As a model system, three diethynyl-substituted triptycenes were synthesized: non-dipolar **1a**, dipolar **1b** bearing a single dipole unit, and dipolar **1c** possessing double dipolar blades. Single-crystal X-ray analysis revealed that **1a** forms two dimensional intermeshed structures, and **1b** constructs the analogue intermeshed packing mode. Interestingly, **1c** yields a chiral helical packing structure. These findings demonstrate that the introduction of dipolar units without changing the steric bulkiness can be a promising motif to search new types of intermolecular arrangements in triptycene-based crystalline materials (Fig. 1).

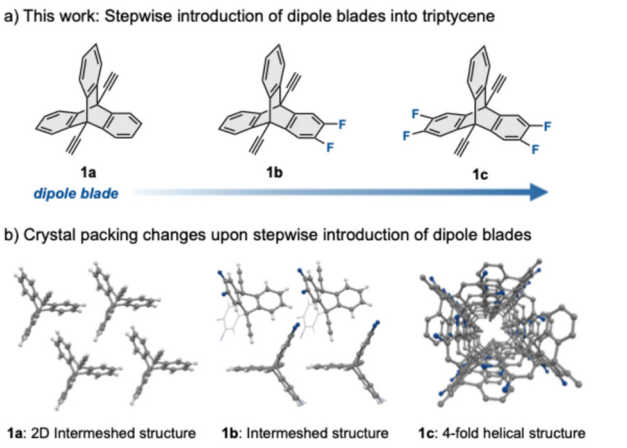

Fig. 1 Illustration of this work: (a) stepwise introduction of dipole blades into triptycene and (b) 2D intermeshed structure of **1a**, 1D intermeshed structure of **1b** and 4-fold helical structure of **1c**.

[a] *Department of Chemistry, Faculty of Science, Hokkaido University, Sapporo, Hokkaido, 060-0810, Japan*
[b] *Department of Chemistry, Faculty of Science, Hokkaido University, Hokkaido 060-0810, Japan*
[c] *Division of Biophysics, Jichi Medical University, Tochigi, 329-0498, Japan*
[d] *Institute for Chemical Reaction Design and Discovery (WPI-ICReDD), Hokkaido University, Hokkaido 001-0021, Japan. E-mail: mingoo@icredd.hokudai.ac.jp*

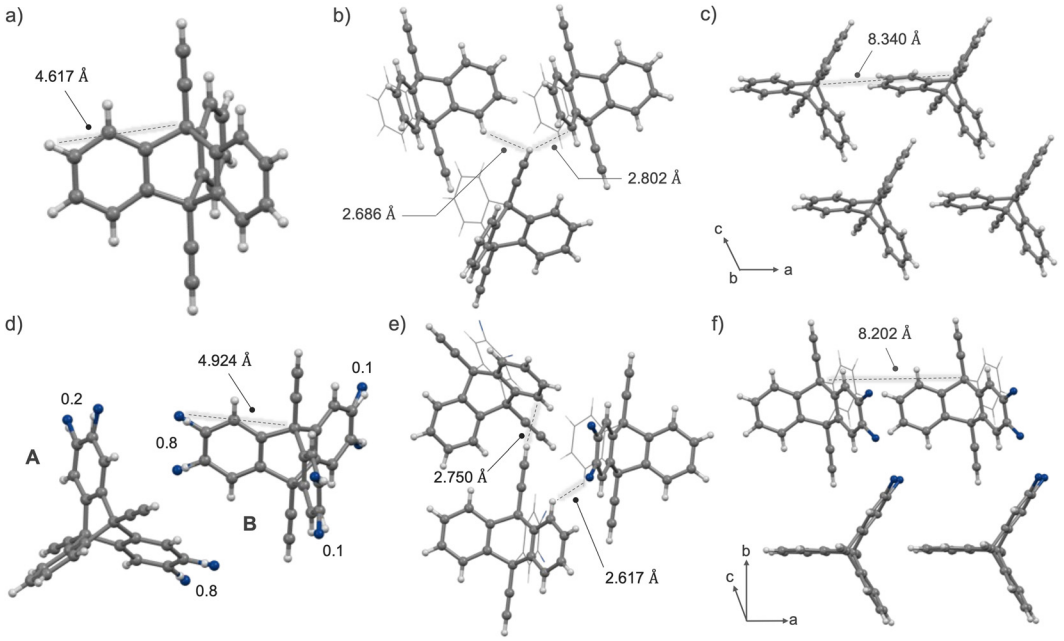

Fig. 2 Crystal structure of **1a**: (a) monomer structure. (b) Close-contact geometry between **1a** units. (c) 2D intermeshed structure. Crystal structure **1b**: (d) two monomer structures having distinct dis-ordered manner. (e) Close-contact geometry between **1b** units. (f) 1D intermeshed structure.

Detailed synthetic protocols are provided in the SI (S3–S8). Fluorinated anthraquinone derivatives **2b** and **2c** were synthesized according to reported procedures.[33,34] Subsequent nucleophilic addition of TIPS-acetylide to **3b** and **3c** afforded the corresponding alkynylated intermediates, which were then subjected to $SnCl_2{\cdot}2H_2O$-mediated reductive aromatization to furnish the fluorinated anthracene derivatives **4b** and **4c**. These anthracenes underwent Diels–Alder cycloaddition with benzyne, generated *in situ* from anthranilic acid and isoamyl nitrite, to yield TIPS-protected dipolar triptycenes **5b** and **5c**. Finally, deprotection of the TIPS groups using TBAF furnished the target dipolar triptycenes **1b** and **1c**. Single crystals suitable for X-ray diffraction analysis were obtained by slow evaporation of diethyl ether solutions. For comparison, the non-dipolar triptycene **1a** was prepared following a literature procedure, and single crystals were similarly grown from diethyl ether.[35] The structures of **1b** and **1c** were confirmed by comprehensive characterization, including ^{1}H and ^{13}C NMR spectroscopy, high-resolution EI mass spectrometry, elemental analysis and single-crystal X-ray diffraction. Further experimental details are available in the SI.

Comparison of the crystal packing structures of **1a–1c** by single-crystal X-ray diffraction revealed that each compound crystallizes in a distinct packing mode (Fig. 2–4). Crystals **1a** and **1b** exhibit intermeshed arrangements of the triptycene frameworks, whereas **1c** adopts a unique fourfold helical packing structure. In the case of non-dipolar triptycene **1a**, an intermeshed structure between adjacent triptycene units was observed (Fig. 2a–c and S1). The crystal of **1a** belongs to the *Cc* space group. The distance between the carbon atom at the 9-position of the triptycene core and the hydrogen atom at the 2-position was 4.617 Å (Fig. 2a). Although no distinct noncovalent interactions were observed between the triptycene units, close contacts were identified, with H···H and C···H separations of 2.686 Å and 2.802 Å, respectively—both slightly shorter than typical van der Waals contact distances. This intermeshed structure extends two-dimensionally along the

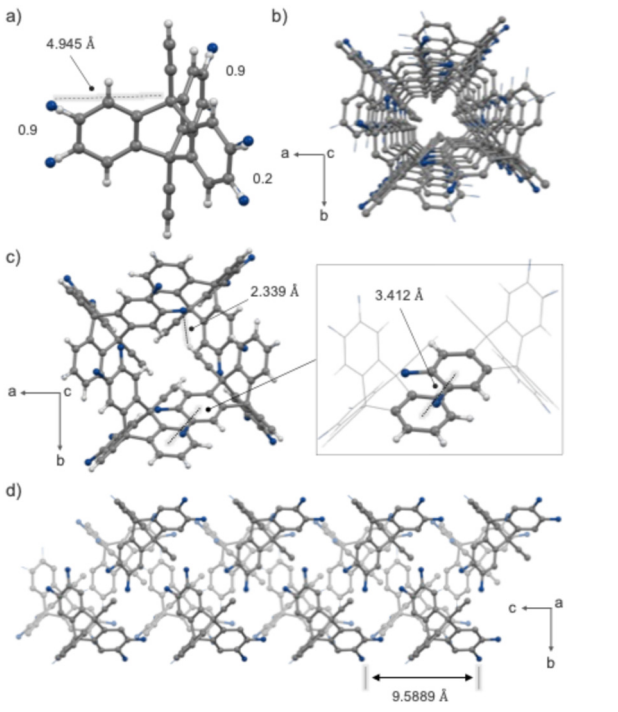

Fig. 3 Crystal structure of **1c** ($P4_1$): (a) monomer structure; (b) top view and (c) side view of *M*-helicity of the 4-fold helical structure; (d) observed π–π interaction and C≡CH···F close contact.

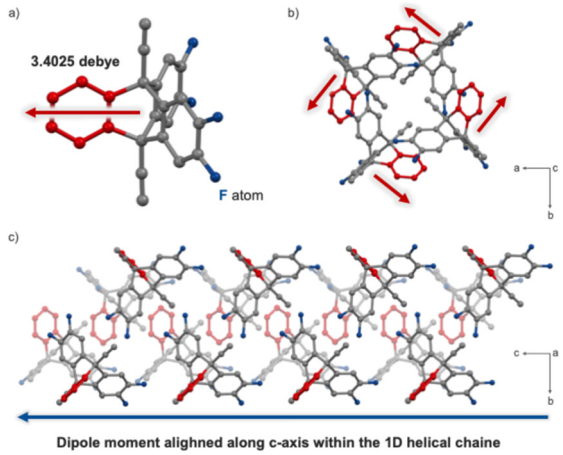

Fig. 4 Calculated dipole moments of the **1c** crystal: (a) monomer and (b) unit cell; (c) illustrations of the dipole moments in the 1D helical structure.

bc-plane, with an interaxial distance between adjacent triptycene units of 8.340 Å (Fig. 2c and S7). Furthermore, these two-dimensional intermeshed layers are stacked in a zigzag fashion along the *b*-axis (Fig. S7).

Dipolar triptycene **1b**, bearing fluorine atoms at the 2,3-positions, crystallized in the $P2_1/c$ space group and exhibited a one-dimensional intermeshed structure (Fig. 2e–g and S8). The distance between the carbon atom at the 9-position of the triptycene core and the fluorine atom at the 2-position was 4.924 Å, indicating a slight elongation compared to **1a** (Fig. 2e). Disorder was observed in the fluorinated phenylene moieties. Two crystallographically independent molecules (A and B) are present in the asymmetric unit (Fig. 2e). In molecule A, the fluorine atom is disordered over two blades (0.80/0.20), while in molecule B it is distributed over three blades (0.80/0.10/0.10). H···F contacts were identified at a distance of 2.617 Å, while adjacent C···H contacts were measured at 2.750 Å. Whereas **1a** forms a two-dimensional intermeshed array of triptycene units, **1b** exhibits a one-dimensional intermeshed arrangement (Fig. 2g and S8). The interaxial distance between fluorinated triptycene units was measured to be 8.202 Å, slightly shorter than that in **1a**. Additionally, the one-dimensional intermeshed columns are stacked along the *b*-axis (Fig. S8).

Interestingly, the crystal of dipolar triptycene **1c**, bearing fluorine atoms at the 2,3,6,7-positions, formed a 4-fold helical chain structure with one-dimensional porous packing in the chiral $P4_1$ space group, which is markedly different from the packing modes of crystals **1a** and **1b** (Fig. 3 and S9). The fluorine atoms were modelled as disordered over the three blades of the triptycene unit, with site occupancies of 0.90, 0.90, and 0.20, indicating minor disorder of the fluorine atom onto the non-fluorinated blade. The distance between the carbon atom at the 9-position of the triptycene core and the fluorine atom at the 2-position was 4.945 Å, comparable to that observed in compound **1b** (Fig. 3a). In this 4-fold helical structure, π–π stacking was observed between the phenylene and fluorinated phenylene rings, with an interplanar distance of 3.412 Å (Fig. 3c). The dihedral angle between these two rings was measured to be 1.74°, indicating that they are nearly parallel (Fig. S9a). In addition, an C≡CH···F close contact was observed at 2.339 Å (Fig. 3c). In the crystal structure of **1c**, the helical columns are arranged side by side with the same helical handedness (Fig. S9b). As a result, the molecular dipoles align in parallel rather than in an antiparallel fashion, so the overall dipole moments are not cancelled out. The helical pitch along the *c*-axis was determined to be 9.5889 Å (Fig. 3d). The four-fold helical structure in the $P4_1$ space group exhibited *P*-helicity, as defined by the orientation of the non-fluorinated phenylene rings. A crystal of **1c** exhibiting the opposite helicity (*M*-helicity) was also observed in distinct crystal particle, corresponding to the chiral $P4_3$ space group (Fig. S10).

To investigate the dipole arrangements in crystals **1a**–**1c**, dipole moments were calculated using density functional theory (DFT) at the B3LYP-D3/6-311+G(d,p) level (Fig. 4 and S11 and S12). At the monomer level, the calculated dipole moments indicated a negligible value of 0.0376 D for **1a**, whereas **1b** and **1c** exhibited comparable dipole moments of 3.2584 D and 3.4025 D, respectively (Fig. 4a and S11). The dipole vector of monomer **1b** was oriented opposite to the fluorinated phenylene unit, whereas in **1c**, it was directed toward the non-fluorinated phenylene unit (Fig. 4a and S11b and c). At the crystal level, the orientations of the dipole moments within the unit cells of dipolar **1b** and **1c** were examined. In the case of **1b**, although each monomer possessed a substantial dipole moment, the spatial arrangement of molecules in the crystal lattice resulted in antiparallel alignment, leading to complete cancellation of the dipole moments within the unit cell (Fig. S12a). In contrast, in crystal **1c**, the molecular dipoles were aligned parallel to each other along the *c*-axis without mutual cancellation, resulting in a net dipole moment of 4.6221 D directed along this axis (Fig. 4 and S12b). This parallel alignment gives rise to a one-dimensional helical polar structure within the crystal (Fig. 4c).

To further rationalize the distinct packing behaviors of **1b** and **1c**, non-covalent intermolecular interactions in the crystals were analyzed using the Independent Gradient Model based on Hirshfeld partition (IGMH) (Fig. S13). The IGMH analysis suggests that the packing of **1b** is not governed by any specific dominant directional intermolecular interactions and is instead largely dominated by isotropic dispersion forces (Fig. S13a). In contrast, **1c** exhibits clear signatures of directional interactions, including π–π stacking and C–H···F hydrogen bonding, which are likely to cooperatively stabilize its polar helical packing structure (Fig. S13b). On this basis, a qualitative energetic picture emerges in which dipole cancellation in **1b** effectively reduces electrostatic contributions to the packing, whereas in **1c**, the absence of dipole cancellation leads to a greater reliance on directional intermolecular interactions to stabilize the crystal structure. In addition to dipole alignment effects, the higher fluorine content in **1c** compared to **1b** may further increase the probability of forming weak but directional intermolecular interactions such as C–H···F hydrogen bonding, thereby

providing additional opportunities for stabilizing the observed interaction network. While molecular dipoles in crystals generally tend to cancel out, the present system shows that increasing dipole multiplicity can promote directional interaction-driven packing, offering a viable strategy for constructing dipolar molecular crystals.

In summary, we investigated the effect of stepwise dipole blades on the crystal packing of diethynylated triptycene derivatives without a dramatic change of the bulkiness. Three molecules—**1a** (non-dipolar), **1b** (single dipole blade), and **1c** (double dipole blades)—were synthesized and their crystal structures were compared. X-ray crystallography revealed that while **1a** and **1b** both form similar intermeshed packing structures, **1c** adopts a 4-fold helical arrangement. Remarkably, in the case of **1c**, the dipole moments are preserved without mutual cancellation within the crystal, leading to the formation of a helical polar structure. These insights show that the dipoles in triptycene can open the variety of intermolecular packing modes even without introducing bulky functional groups.

Conflicts of interest

There are no conflicts to declare.

Data availability

The data supporting this article have been included as part of the supplementary information (SI).

Supplementary information is available. See DOI: https://doi.org/10.1039/d6ce00126b.

CCDC 2493850–2493853 contain the supplementary crystallographic data for this paper.[36a–d]

Acknowledgements

This work was financially supported by the Japan Society for the Promotion of Science (JSPS) *via* KAKENHI grants JP25K00073; by the JST *via* FOREST grant JPMJFR232C; and by the Institute for Chemical Reaction Design and Discovery (ICReDD), established by the World Premier International Research Initiative (WPI), MEXT, Japan. XRD studies were additionally performed at the beamline AR-NW12A of the Photon Factory under PF-PAC proposal numbers 2024G039.

Notes and references

1 N. P. D. Bartlett, M. J. Ryan and S. G. Cohen, *J. Am. Chem. Soc.*, 1942, **64**, 2649–2653.
2 (*a*) N. Seiki, Y. Shoji, T. Kajitani, F. Ishiwari, A. Kosaka, T. Hikima, M. Takata, T. Someya and T. Fukushima, *Science*, 2015, **348**, 1122–1126; (*b*) F. K.-C. Leung, F. Ishiwari, T. Kajitani, Y. Shoji, T. Hikima, M. Takata, A. Saeki, S. Seki, Y. M. A. Yamada and T. Fukushima, *J. Am. Chem. Soc.*, 2016, **138**, 11727–11733.
3 (*a*) A. Alam, A. Hassan and N. Das, *Prog. Mater. Sci.*, 2026, **155**, 101528; (*b*) M.-J. Gu, Y.-F. Wang, Y. Han and C.-F. Chen, *Org. Biomol. Chem.*, 2021, **19**, 10047–10067.
4 M. Zharnikov, Y. Shoji and T. Fukushima, *Acc. Chem. Res.*, 2025, **58**, 312–324.
5 J.-S. Yang, C.-P. Liu, B.-C. Lin, C.-W. Tu and G.-H. Lee, *J. Org. Chem.*, 2002, **67**, 7343–7354.
6 K. Yamamura, T. Kawashima, K. Eda, F. Tajima and M. Hashimoto, *J. Mol. Struct.*, 2005, **737**, 1–6.
7 C. Zhang and C.-F. Chen, *J. Org. Chem.*, 2006, **71**, 6626–6629.
8 C. Zhang and C. F. Chen, *CrystEngComm*, 2010, **12**, 3255–3261.
9 P.-F. Li and C.-F. Chen, *J. Org. Chem.*, 2012, **77**, 9250–9259.
10 M. Mastalerz and I. M. Oppel, *Angew. Chem., Int. Ed.*, 2012, **51**, 5252–5255.
11 Y. Han, Y. Jiang and C.-F. Chen, *Chin. Chem. Lett.*, 2013, **24**, 475–478.
12 N. G. White and M. J. MacLachlan, *Chem. Sci.*, 2015, **6**, 6245–6249.
13 N. G. White and M. J. MacLachlan, *Cryst. Growth Des.*, 2015, **15**, 5629–5636.
14 G. Zhang, F. Rominger and M. Mastalerz, *Cryst. Growth Des.*, 2016, **16**, 5542–5548.
15 S. Greatorex and M. A. Halcrow, *CrystEngComm*, 2016, **18**, 4695–4698.
16 S. Langis-Barsetti, T. Maris and J. D. Wuest, *J. Org. Chem.*, 2018, **83**, 15426–15437.
17 P. Li, P. Li, M. R. Ryder, Z. Liu, C. L. Stern, O. K. Farha and J. F. Stoddart, *Angew. Chem., Int. Ed.*, 2019, **58**, 1664–1669.
18 N. Tanaka, Y. Inagaki, K. Yamaguchi and W. Setaka, *Cryst. Growth Des.*, 2020, **20**, 1097–1102.
19 Y. Takemasa and K. Nozaki, *J. Org. Chem.*, 2022, **87**, 1502–1506.
20 T. Furuta, K. Oka and N. Tohnai, *Bull. Chem. Soc. Jpn.*, 2024, **97**, uoae013.
21 A. Dua, H. M. Titi, H. K. Sharma and S. Roy, *J. Struct. Chem.*, 2024, **65**, 958–966.
22 W. Murakami, T. Kitayama, Y. Chiba, H. Moteki, R. Shirato, K. Iwase, R. Toyoda, R. Sakamoto and S. Takaishi, *J. Mater. Chem. A*, 2025, **13**, 25724–25731.
23 M. O'Shaughnessy, H. Qu, X. Wang, J. B. Holmes, L. Emsley, J. Glover, R. Hafizi, G. M. Day and A. I. Cooper, *J. Am. Chem. Soc.*, 2025, **147**, 39351–39358.
24 A. Bashir-Hashemi, H. Hart and D. L. Ward, *J. Am. Chem. Soc.*, 1986, **108**, 6675–6679.
25 A. Wiehe, M. O. Senge and H. Kurreck, *Liebigs Ann. Org. Bioorg. Chem.*, 1997, **1997**, 1951–1963.
26 J. Lu, J. Zhang, X. Shen, D. M. Ho and R. A. Pascal Jr, *J. Am. Chem. Soc.*, 2002, **124**, 8035–8041.
27 V. J. Chebny, T. S. Navale, R. Shukla, S. V. Lindeman and R. Rathore, *Org. Lett.*, 2009, **11**, 2253–2256.
28 Y. Shuku, A. Mizuno, R. Ushiroguchi, C. S. Hyun, Y. J. Ryu, B.-K. An, J. E. Kwon, S. Y. Park, M. Tsuchiizu and K. Awaga, *Chem. Commun.*, 2018, **54**, 3815–3818.
29 Y. Shoji, S. Yamamoto and T. Fukushima, *Chem. Lett.*, 2021, **50**, 1240–1243.
30 B. Kohl, L. C. Over, T. Lohr, M. Vasylyeva, F. Rominger and M. Mastalerz, *Org. Lett.*, 2014, **16**, 5596–5599.

31 W. Yang, R. Jiang, C. Liu, B. Yu, X. Cai and H. Wang, *Cryst. Growth Des.*, 2021, **21**, 6497–6503.
32 K. Reichenbächer, H. I. Süss and J. Hulliger, *Chem. Soc. Rev.*, 2005, **34**, 22–30.
33 H. Hayashi, N. Aratani and H. Yamada, *Chemistry*, 2017, **23**, 7000–7008.
34 S. N. Afraj, B.-H. Jiang, Y.-W. Su, C.-H. Yang, H.-S. Shih, A. Velusamy, J.-S. Ni, Y. Ezhumalai, T.-Y. Su, C.-L. Liu, S. Yau, C.-P. Chen and M.-C. Chen, *J. Mater. Chem. C*, 2024, **12**, 2247–2257.
35 A. M. Sirven, R. Garbage, Y. Qiao, C. Kammerer and G. Rapenne, *Chemistry*, 2015, **21**, 15013–15019.
36 (*a*) CCDC 2493850: Experimental Crystal Structure Determination, 2026, DOI: 10.5517/ccdc.csd.cc2pq1s8; (*b*) CCDC 2493851: Experimental Crystal Structure Determination, 2026, DOI: 10.5517/ccdc.csd.cc2pq1t9; (*c*) CCDC 2493852: Experimental Crystal Structure Determination, 2026, DOI: 10.5517/ccdc.csd.cc2pq1vb; (*d*) CCDC 2493853: Experimental Crystal Structure Determination, 2026, DOI: 10.5517/ccdc.csd.cc2pq1wc.